The Astrophysical Journal Letters, 933:L30 (7pp), 2022 July 10 https://doi.org/10.3847/2041-8213/ac7c72

Viability of Novae as Sources of Galactic Lithium

Alex J. Kemp[1,2], Amanda I. Karakas[1,2], Andrew R. Casey[1,2], Benoit Côté[3,4], Robert G. Izzard[5], and Zara Osborn[1,2]
[1] School of Physics & Astronomy, Monash University, Clayton 3800, Victoria, Australia; alexander.kemp@monash.edu
[2] Centre of Excellence for Astrophysics in Three Dimensions (ASTRO-3D), Melbourne, Victoria, Australia
[3] Department of Physics and Astronomy, University of Victoria, Victoria, BC V8P 5C2, Canada
[4] Konkoly Observatory, Research Centre for Astronomy and Earth Sciences, Eötvös Loránd Research Network (ELKH), Konkoly Thege Miklós út 15-17, H-1121 Budapest, Hungary
[5] Astrophysics Research Group, University of Surrey, Guildford, Surrey GU2 7XH, UK
Received 2022 May 25; revised 2022 June 26; accepted 2022 June 27; published 2022 July 7

Abstract

Of all the light elements, the evolution of lithium (Li) in the Milky Way is perhaps the most difficult to explain. Li is difficult to synthesize and is easily destroyed, making most stellar sites unsuitable for producing Li in sufficient quantities to account for the protosolar abundance. For decades, novae have been proposed as a potential explanation for this "Galactic Li problem," and the recent detection of ^{7}Be in the ejecta of multiple nova eruptions has breathed new life into this theory. In this work, we assess the viability of novae as dominant producers of Li in the Milky Way. We present the most comprehensive treatment of novae in a galactic chemical evolution code to date, testing theoretically and observationally derived nova Li yields by integrating metallicity-dependent nova ejecta profiles computed using the binary population synthesis code `binary_c` with the galactic chemical evolution code `OMEGA+`. We find that our galactic chemical evolution models which use observationally derived Li yields account for the protosolar Li abundance very well, while models relying on theoretical nova yields cannot reproduce the protosolar observation. A brief exploration of physical uncertainties including single-stellar yields, the metallicity resolution of our nova treatment, common-envelope physics, and nova accretion efficiencies indicates that this result is robust to physical assumptions. Scatter within the observationally derived Li yields in novae is identified as the primary source of uncertainty, motivating further observations of ^{7}Be in nova ejecta.

Unified Astronomy Thesaurus concepts: Classical novae (251); Nucleosynthesis (1131); Stellar nucleosynthesis (1616); Galactic abundances (2002)

1. Introduction

Lithium (Li) is a notoriously troublesome element. It is extremely fragile, destroyed in H-capture reactions at temperatures as low as 2×10^{6} K. This is cool enough for stars to deplete their surface Li on, or before, the main sequence by convecting surface material deeper into the star where the Li is destroyed. This makes it almost impossible to accurately calculate the Li abundance at birth for most stars. The exception to this is the Sun, for which we have access to meteorites that preserve the protosolar Li abundance (A(Li) $= 3.26 \pm 0.05$; see Asplund et al. 2009; Lodders et al. 2009). Galactic chemical evolution (GCE) models typically underproduce this Li abundance by roughly an order of magnitude, a discrepancy known as the "Galactic Li problem" (D'Antona & Matteucci 1991; Matteucci et al. 1995).

The fragility of Li is detrimental to its production. Its dominant isotope ^{7}Li is formed as the sole decay product of ^{7}Be, which is unstable with a half-life of 53.3 days. ^{7}Be forms via proton–proton (pp) chains during H burning but quickly decays to ^{7}Li via electron capture (pp II). The ^{7}Li itself is then also destroyed by proton capture, with the net result that very little survives H burning. The Cameron–Fowler mechanism (Cameron & Fowler 1971) proposes that some of the ^{7}Be is transported to a cooler region, where electron captures and the natural decay of ^{7}Be can form Li in an environment where it can survive.

Although the yield is model dependent, relatively little Li can be produced in this way by AGB stars (e.g., Karakas 2010; Pignatari et al. 2016), and core-collapse supernova models produce orders of magnitude less (e.g., Kobayashi et al. 2006). Li can also be produced through spallation reactions caused by cosmic rays at levels comparable to AGB stars (Prantzos 2012).

It has been proposed for many years now that classical novae could be viable sites for Li production (Arnould & Norgaard 1975). Novae are transients caused by explosive H-burning episodes on the surface of accreting white dwarfs (WDs). Their high burning temperatures, rapid evolution, and high mass-loss rates during outburst make them promising Li producers due to their ability to synthesize ^{7}Be in significant quantities and then transport that material into cooler mass-losing regions during outburst, where it can decay to ^{7}Li without that Li being destroyed. Early theoretical work on explosive H burning and nova yields found significant overproduction of Li relative to solar-composition material (Arnould & Norgaard 1975; Starrfield et al. 1978). More sophisticated modeling with comprehensive reaction networks qualitatively confirmed these early results (José & Hernanz 1998; Starrfield et al. 2000), solidifying the idea of novae as Li factories.

Since the first detection of ^{7}Be in 2015 (Tajitsu et al. 2015), ^{7}Be has been detected in the spectra of a handful of nova outbursts (Tajitsu et al. 2015; Molaro et al. 2016; Tajitsu et al. 2016; Selvelli et al. 2018; Molaro et al. 2020; Arai et al. 2021; Izzo et al. 2022). These observations not only provided direct evidence of novae producing Li but also implied a far greater

overproduction factor than that found in theoretical models, reigniting interest in novae as a solution to the Galactic Li problem. Where older chemical evolution models that relied on theoretical nova yields identified novae as promising candidates (Romano et al. 2001), newer works making use of the observationally derived yields demonstrated that novae could account for the high protosolar Li abundance (Cescutti & Molaro 2019; Grisoni et al. 2019).

However, existing calculations on the viability of novae as dominant sources of Li have relied upon simplified models for how novae behave. For example, the recent work of Grisoni et al. (2019) assumes each nova system to undergo 10^4 eruptions (Bath & Shaviv 1978), assigning each a constant ejecta mass of Li bounded by observations of V1369 Cen (Izzo et al. 2015). The birth rate of nova systems is set as a fraction of the WD formation rate, and all nova eruptions generated from a period of star formation are assumed to occur instantaneously, offset by a fixed amount of time. Cescutti & Molaro (2019) features a more sophisticated treatment that approximates the continuous release of nova ejecta and instead treats the average Li ejecta mass per event as a free parameter, ultimately determined to be consistent with observations of ^{7}Be in nova ejecta. These assumptions were necessary as more sophisticated models for nova populations did not exist.

In this work, we instead rely on the results of previously computed theoretical nova populations (Kemp et al. 2022), where each nova eruption is treated individually based on the white dwarf mass $M_{\rm WD}$ and accretion rate $\dot{M}$. Our chemical evolution model and treatment of novae are described in Section 2, our findings on novae as sources of Li in the Milky Way are presented in Section 3, and commentary on the significance and uncertainty in our findings is presented in Section 4. We conclude in Section 5. Supplementary material can be accessed here: doi:10.5281/zenodo.6644271.

2. Methodology

2.1. Nova Treatment

Figure 1 shows a nova delay-time (upper panel) and ejecta delay-time (lower panel) distribution colored by the WD composition. The delay-time distribution tracks the time from star formation to each nova eruption, where each nova eruption is weighted equally. The ejecta delay-time distribution instead weights each nova eruption by the total mass ejected into the interstellar medium, tracking the mass ejection profile of novae for each burst of star formation.

A metallicity-dependent grid of these precomputed ejecta delay-time distributions is taken as a direct input into our galactic chemical evolution models. The underlying binary population synthesis models are a subset ($Z = 10^{-4}$, 10^{-3}, 5×10^{-3}, 0.01, 0.02) of those presented in Kemp et al. (2022), and further details about the process of simulating each nova eruption in `binary_c` (Izzard et al. 2004, 2006, 2009, 2018) are available in Kemp et al. (2021).

To make predictions about specific elements or isotopes, these ejecta delay-time distributions must be combined with nova-yield tables. We can divide our nova population according to the white dwarf mass $M_{\rm WD}$ and accretion rate $\dot{M}$ at the time of eruption by using an array of ejecta delay-time distributions that correspond to different regions of $M_{\rm WD}$–$\dot{M}$ parameter space. This allows us to map physics-dependent yields from theoretical models (José & Hernanz 1998; Starrfield et al. 2009; Rukeya et al. 2017; Starrfield et al. 2020; José et al. 2022) to their relevant ejecta delay-time distributions. This treatment innately accounts for ejecta mass and delay-time variation in different nova systems, the metallicity dependence of nova-system formation and evolution, and physics-dependent aspects of nova nucleosynthesis (Iliadis 2015).

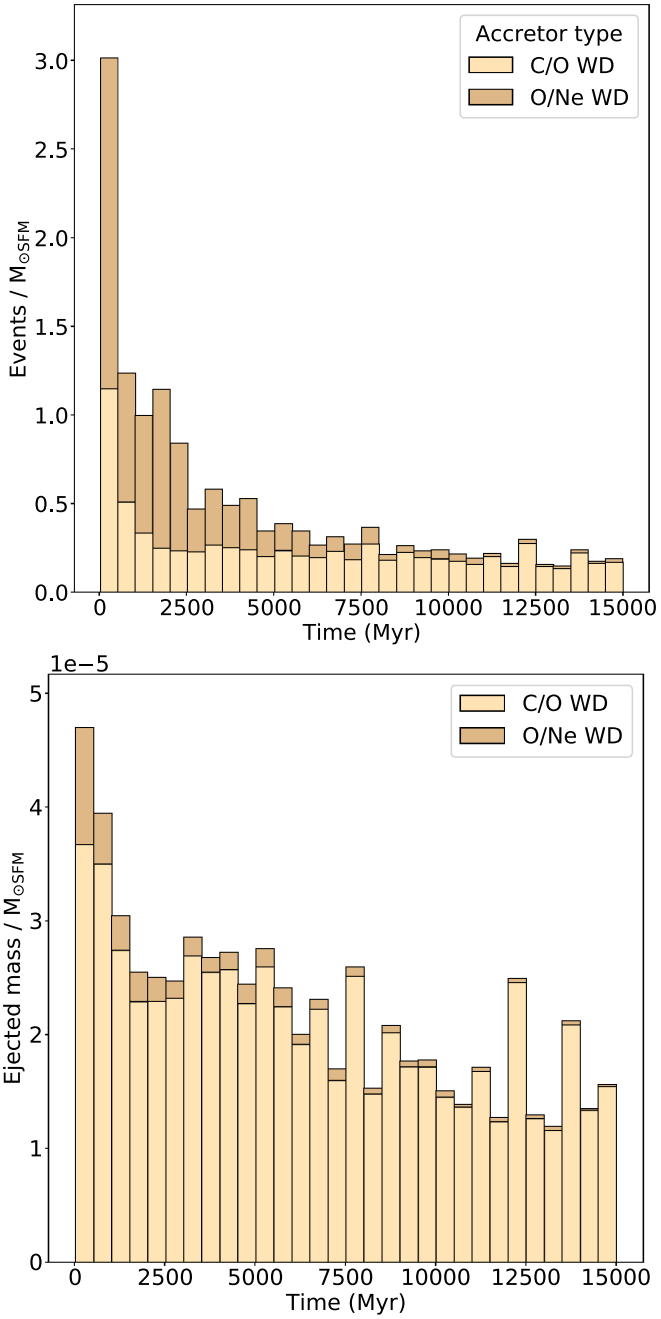

Figure 1. Delay-time (upper panel, tracking when the nova eruptions occur relative to star formation) and ejecta delay-time (lower panel, tracking when mass is ejected relative to star formation) distributions for $Z = 10^{-3}$. Both distributions are normalized per solar mass of star-forming material $M_{\odot\rm SFM}$ (for details, see Kemp et al. 2021, 2022).

2.2. Nova-yield Sets

We have compiled five theoretical nova nucleosynthesis yield profiles. The implementation of each of these yield profiles is described below:

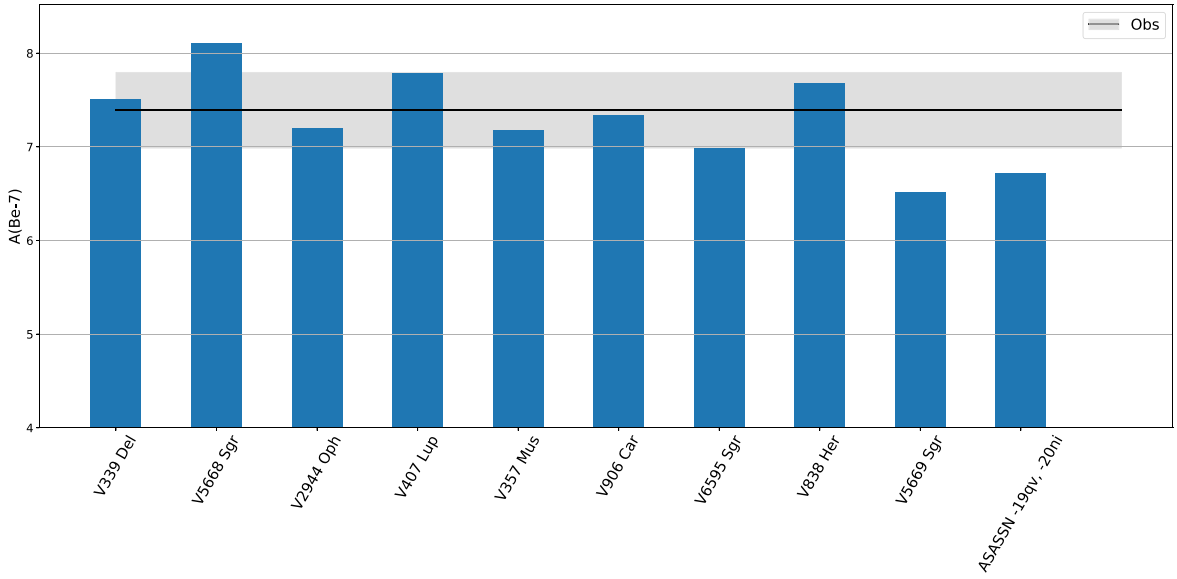

Figure 2. Observationally derived $A(^7\mathrm{Be})$, corrected for ^{7}Be decay since eruption. Decay-corrected $A(^7\mathrm{Be})$ values are taken from Molaro et al. (2020) Table 1 (V339 Del, V5668 Sgr, V2944 Oph, V407 Lup, V357 Mus, V906 Car), Molaro et al. (2022) table 4 (V6595 Sgr, V838 Her, V5669 Sgr), and Izzo et al. (2022) (ASASSN-19qv, ASASSN-20ni).

1. J1998: Makes use of 50% pre-enriched C/O WD nucleosynthesis yields for $M_{\mathrm{WD}} = 0.8$ and 1.0 $M_{\odot}$, and 50% pre-enriched O/Ne WD yields for $M_{\mathrm{WD}} = 1.15$, 1.25, and 1.35 $\mathrm{M}_{\odot}$ (José & Hernanz 1998).
2. S2009/2020: Makes use of 50% pre-enriched C/O WD nucleosynthesis yields for $M_{\mathrm{WD}} = 0.6$, 0.8, 1.0, and 1.15 $\mathrm{M}_{\odot}$ (Starrfield et al. 2020), and 50% pre-enriched O/Ne WD yields for $M_{\mathrm{WD}} = 1.25$ and 1.35 $\mathrm{M}_{\odot}$ (Starrfield et al. 2009).
3. J2020: Makes use of C/O WD nucleosynthesis yields for $M_{\mathrm{WD}} = 1.0$ $\mathrm{M}_{\odot}$ and O/Ne WD yields for $M_{\mathrm{WD}} = 1.15$ $\mathrm{M}_{\odot}$ (José et al. 2022). Rather than assuming a pre-enrichment fraction to account for mixing during the eruption, these yields come from models that instead simulate the eruption by combining 3D (FLASH; Fryxell et al. 2000) and 1D (SHIVA; José & Hernanz 1998) methods to model the conditions at outburst.
4. R2017: Makes use of 50% pre-enriched Li yields for C/O WDs at $M_{\mathrm{WD}} = 0.51$, 0.6, 0.7, 0.8, 0.9, and 1.0, and 50% pre-enriched O/Ne WD yields for $M_{\mathrm{WD}} = 1.1$, 1.2, 1.3, and 1.34 $\mathrm{M}_{\odot}$ (Rukeya et al. 2017). This yield profile is notable for also providing yields for a range of accretion rates for each M_{WD}, rather than sampling only at a fixed accretion rate of 2×10^{-10} $\mathrm{M}_{\odot}\,\mathrm{yr}^{-1}$ as in the previously described J1998, S2009/2020, and J2020 sets. A figure demonstrating the breakdown of this grid is provided in the supplementary material.
5. R2017simple: Makes use of 50% pre-enriched Li yields for C/O WDs at $M_{\mathrm{WD}} = 0.8$ and 1.0 $M_{\odot}$, and O/Ne WD yields for $M_{\mathrm{WD}} = 1.15$, 1.25, and 1.35 $\mathrm{M}_{\odot}$ (Rukeya et al. 2017). This yield set is, by design, identical to the parameter space set out in the J1998 set. It is useful as it can be directly compared with the R2017 set to assess the impact of only sampling the accretion-rate space at 2×10^{-10} $M_{\odot}\,\mathrm{yr}^{-1}$.

Note that all of the underlying models informing the above theoretical yield profiles assume solar-composition material.

Figure 2 presents all available observationally derived ^{7}Be abundances $A(^7\mathrm{Be})$, corrected for ^{7}Be decay (Molaro et al. 2020, 2022). Overplotted are the mean and 1σ error bars for these data computed using all available observations ($A(^7\mathrm{Be}) = 7.12 \pm 0.71$, gray). The H mass fraction X of the ejecta is required to convert this information into a useful mass fraction of ^{7}Be, a quantity dependent on the fraction of core material mixed into the burning zone, which we must assume. We assess the impact of this assumption by considering two cases for the mixing fraction, 50% ($X = 0.35$) and 25% ($X = 0.5$), with the associated X values for these two cases based on the simulations of José & Hernanz (1998) and Starrfield et al. (2009, 2020).

Significant scatter exists in these measurements. The novae V407 Lup, V6595 Sgr, and V838 Her are classified as O/Ne novae due to the detection of bright Ne lines in their late nebula phases (Table 4 in Molaro et al. 2022). Of these novae, only V407 Lup and V838 Her have measurements notably above average. The dusty nova V5668 Sgr has the highest value ($A(^7\mathrm{Be}) = 8.1$), but V357 Mus and V906 Car appear typical despite also being dusty (Gordon et al. 2021 and references therein).

2.3. Milky Way Chemical Evolution Model

Our chemical evolution model is computed using the two-zone GCE code OMEGA+ (Côté et al. 2018). The model structure consists of a star-forming galactic component coupled with a circumgalactic halo that functions as a hot gas reservoir and facilitates galactic recycling. The central galactic component is simulated using OMEGA (Côté et al. 2017), a one-zone GCE code accounting for the chemical yields of different stellar populations.

Our baseline Milky Way model, to which we add nova contributions, uses an exponential Galactic inflow rate and calculates outflows as a function of star formation. Stellar yields for Type Ia supernovae and asymptotic giant branch (AGB) and massive stars are taken from Thielemann et al. (1986), Karakas (2010), and Kobayashi et al. (2006),

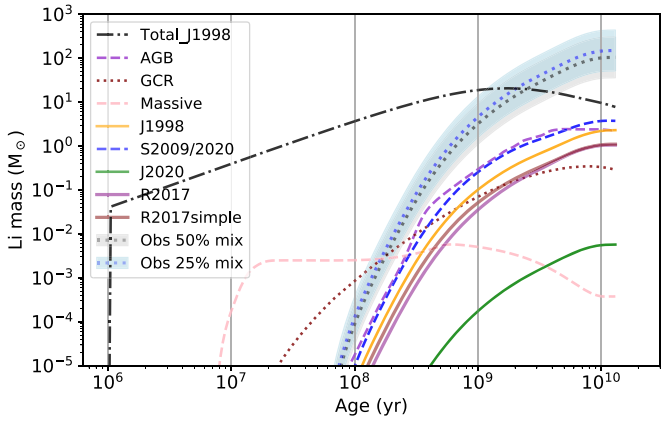

Figure 3. Li mass contributions from different sources as a function of Galactic age. See main text for discussion.

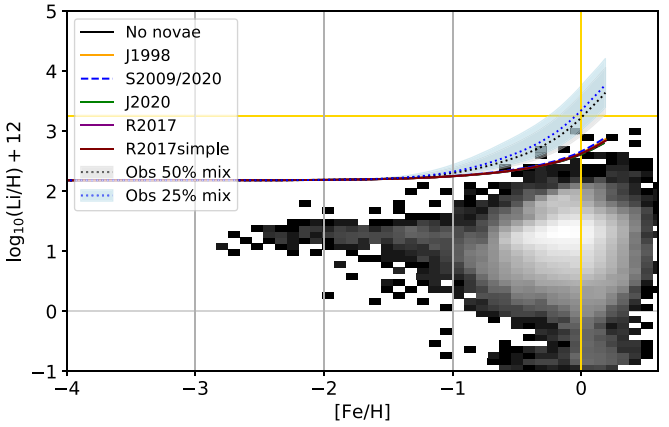

Figure 4. Li abundance vs. [Fe/H] in our Galactic models, overlaid with the protosolar Li abundance (Lodders et al. 2009) (yellow cross-hair) and Li abundance data from GALAH DR3 (Buder et al. 2021). All models include AGB, massive stellar, and GCR sources in addition to the designated nova yield set.

respectively. Contributions to Li production from cosmic rays are approximated as a function of [Fe/H] using data from Figure 16 of Prantzos (2012).

Further details and figures used to validate our baseline Milky Way model can be found in the supplementary material.

3. Results

3.1. Lithium Source Comparison

Figure 3 presents the mass of Li produced by different sources as a function of Galactic age. The total mass of Li for the full J1998 GCE model is shown for comparison, which includes primordial material being introduced through galactic inflows as well as AGB, massive stellar, Galactic cosmic-ray (GCR), and nova contributions using the previously described J1998 yield profile.

Two different models relying on different observationally derived yield sets are shown (dotted lines + shaded 1σ error bar): assuming 50% mixing of underlying core material (gray) and assuming 25% mixing (blue). Reducing the mixing fraction from 50% to 25% is seen to increase the average noticeably, although the change is small relative to the observational uncertainty. Despite the large error bars resulting from the scatter in observational Li determinations, it is clear that even in the most pessimistic case, novae are expected to produce far more Li than any other stellar source over the galaxy's lifetime.

The S2009/2020 yield set results in the most Li produced by novae when theoretical nova yields are used, but even this yield set produces almost an order of magnitude less Li by $t = 10$ Gyr than the lowest error bound of the observational yield sets. The disagreement between theoretical models of Li production in novae and observations of Li in the ejecta is at least a factor of 5.

Comparing the different theoretical nova-yield profiles, the profiles relying on premixing—J1998, S2009/2020, R2017, R2017simple—have broadly comparable productivity, overtaking GCR contributions after roughly 2 Gyr of evolution but never overproducing relative to AGB yields by more than a factor of 2 (S2009/2020). Note that the R2017 and R2017simple models are almost identical in Figure 3, but there is discernible variation between the Li masses produced by yield profiles from different research groups. This strongly implies that not resolving the accretion-rate dependency of nova nucleosynthesis is of secondary importance. A figure presenting the distribution of Li mass production in $M_{\rm WD}$–$\dot{M}$ space according to the R2017 model is included in the supplementary material.

The only theoretical yield set that does not rely on premixing —J2020—produces three orders of magnitude less Li than the theoretical pre-enriched yield sets. José et al. (2022) attribute this to the longer timescale over which thermonuclear runaway develops in these models, which allows far more ^{7}Be to be destroyed before it can be advected to cooler regions. A more detailed discussion is presented in José et al. (2022).

3.2. Lithium in the Milky Way

Figure 4 presents the Li abundance versus [Fe/H] in each of our Galactic models, overlaid with the protosolar Li abundance (yellow) and Li abundances of stars in GALAH DR3 (Buder et al. 2021, gray scale). The GALAH data set used is comprised of the 85,490 main-sequence stars (`logg` > 3.7) that had acceptable signal-to-noise ratios (`snr_c3_iraf` > 30), stellar parameters (`flag_sp` $= 0$), and Fe/H (`flag_fe_h` $= 0$) and Li/Fe (`flag_Li_fe` $= 0$) abundances. Unlike Figure 3, which only plots the contributions specifically from novae in the curves labeled with nova-yield profiles, each of the models in Figure 4 includes the specified nova-yield profile in addition to all non-nova Li sources.

Figure 4 demonstrates that models making use of observationally derived nova Li yields can account for the protosolar Li abundance. Our model relying upon the observational Li yield with the 50% mixing assumption passes cleanly through the protosolar Li observation. The Li mass fraction for novae used in this GCE model is approximately 4.8×10^{-5}, which we present as our empirical solution for the average Li mass fraction in nova ejecta. However, note that the model assuming 25% mixing produces a Li abundance at [Fe/H] $= 0$ that lies within 0.1 dex of the protosolar observation, well within the 1σ uncertainties accounting for scattering in the observationally derived $A(^7\mathrm{Be})$ data.

Conversely, all models relying on theoretical yield profiles are indistinguishable from each other or the baseline model without novae. These predict Li abundances an order of magnitude below the protosolar Li abundance. Despite being non-negligible Li producers (Figure 3), according to these yield profiles, novae simply do not produce enough Li to account for

the solar Li abundance or, to a lesser extent, the upper envelope of the GALAH data.

It has been proposed (Grisoni et al. 2019) that the metallicity dependence of novae could explain observations of declining Li abundances at high metallicities, a feature detected in the Milky Way by multiple groups (Mena et al. 2015; Guiglion et al. 2016; Bensby & Lind 2018; Buder et al. 2018; Fu et al. 2018; Buder et al. 2021). We report that none of our models show signs of a Li decline at high metallicity, despite accounting for the metallicity-dependent variation in our nova distributions.

4. Discussion

GCE models incorporate, albeit often indirectly, a vast amount of physics. The adopted yield sets and productivities of different stellar phenomena (e.g., AGB stars, massive stars, Type Ia supernovae, neutron star mergers, etc.) all affect how a simulated galaxy evolves, and each of these prescriptions has its own physical assumptions. Additionally, modeling choices for galactic processes such as the star formation efficiency and inflow and outflow rates are vital. This modeling complexity renders the assessment of uncertainty difficult.

Our baseline model of the Milky Way satisfactorily reproduces a range of observables (see the supplementary material for supporting figures), including key elemental abundance trends. This does not necessarily make the model correct; rather, it is intended to provide a representative baseline model with which we can assess the importance of novae. In this work, we are concerned with Li, an element notoriously sensitive to stellar modeling choices. The two classes of assumptions most likely to affect our results are the adopted non-nova stellar yields and the assumed binary physics behind our ejecta delay-time distributions. We summarize here the results of a brief exploration of both these uncertainties.

We find that changing the adopted AGB yields from Karakas (2010) yields to NuGrid yields (Pignatari et al. 2016) has a minimal effect on the ability of our models using observational nova yield profiles to reproduce the solar Li abundance, despite the NuGrid yields producing roughly twice as much Li from AGB stars by [Fe/H] = 0. Assessing the extreme lower bound, removing all non-nova sources of Li results in a 0.25 dex negative shift relative to the protosolar abundance. This is well within the 1σ bounds associated with the observational data. Preliminary results of an investigation into the statistical effects of binary interactions on solar metallicity AGB yields—an effect neglected in contemporary GCE codes—indicate at most a 15% reduction in Li (Z. Osborn et al. 2022, in preparation). We therefore conclude that our results are likely robust against uncertainties in non-nova Li yields.

Removing the metallicity dependence of the nova ejecta delay-time distributions and instead only using ejecta delay-time distributions computed at $Z = 0.02$ results in a 35% reduction in Li production from novae. This reduces the Li abundance at [Fe/H] = 0 predicted by our GCE models using observationally derived yield sets by 0.3–0.4 dex. The protosolar Li abundance remains comfortably within the 1σ error bars associated with the observationally derived yield profiles. We therefore conclude that our results are robust to the metallicity resolution of our array of nova ejecta delay-time distributions.

A full investigation of the binary uncertainty is beyond the scope of this work. However, as an indicative example,

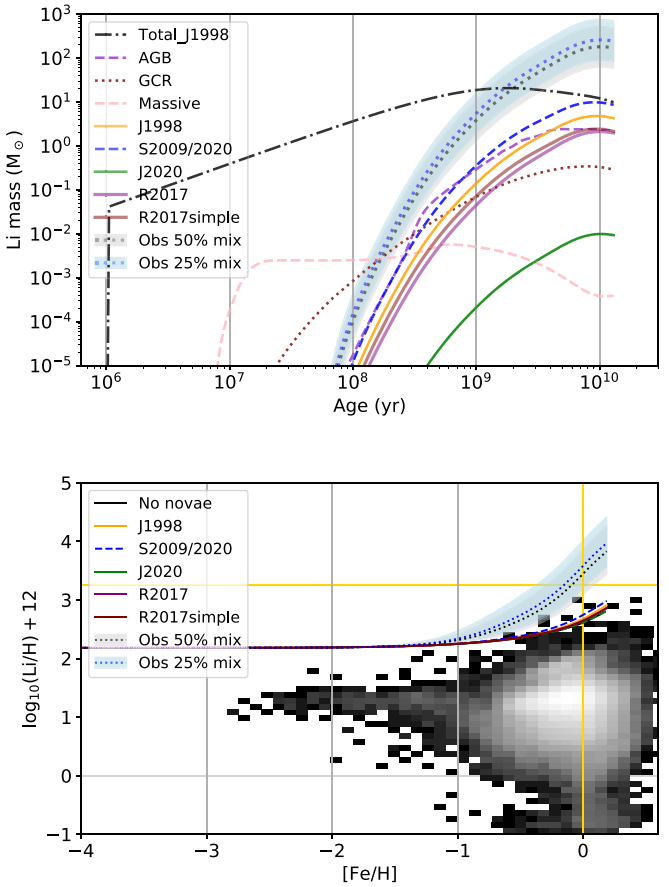

Figure 5. As Figures 3 and 4 when the common-envelope parameter λ_{CE} is set to 0.5, rather than the Wang et al. (2016) prescription used in our baseline case. This physics case doubles the expected nova rate in M31 (Kemp et al. 2021, and we see this reflected in a doubling in Li production). The ability of observationally derived nova yield profiles to reproduce the protosolar Li abundance, and the inability of theoretical yield profiles, appears robust.

Figure 5 presents the results of using an alternative set of ejecta delay-time distributions computed using a different set of binary physics. In producing Figure 5, we have replaced the Wang et al. (2016) prescription for the common-envelope parameter λ_{CE} (Kemp et al. 2021) with a constant value of 0.5. This physics set was found in a previous work (Kemp et al. 2021) to approximately double the predicted nova rate in M31 and represents an extreme case of variation due to binary physics (Kemp et al. 2021). We find that the total mass of Li produced by novae approximately doubles under this assumption, implying roughly a factor of 2 uncertainty in our results from the physical uncertainty in binary stellar physics.

We also investigated the effect of replacing the nova accretion efficiency prescription of Wang (2018) with a constant to assess the potential impact that nova-specific modeling choices could have on our results. Setting the accretion efficiency to 0.01, meaning that in each nova eruption 99% of the accreted material is lost to the WD per eruption, has a negligible effect on our results.

5. Conclusions

In this work, we assess the importance of novae in the synthesis of Li in the Milky Way using the galactic chemical evolution code OMEGA+. Previous galactic chemical evolution models have either relied on simplified treatments of novae or

ignored them altogether. In this work, we employ metallicity-dependent arrays of nova ejecta delay-time distributions computed using the binary population synthesis code `binary_c` to model the Galactic nova population.

We assess the viability of novae in the context of five different theoretical yield profiles (José & Hernanz 1998; Starrfield et al. 2009; Rukeya et al. 2017; Starrfield et al. 2020; José et al. 2022) in addition to observationally derived Li yields (Molaro et al. 2020; Izzo et al. 2022; Molaro et al. 2022). We find that our Galactic chemical evolution models, which make use of observationally derived Li yields, account for the protosolar Li abundance very well, while the models that make use of theoretical yield profiles universally fail to reproduce this observation by an order of magnitude.

We find this result to be robust to all physical uncertainties, which were included in our exploratory analysis, including the choice of AGB yields, the metallicity resolution of our array of nova ejecta delay-time distributions, common-envelope physics, and nova accretion efficiencies. Further, physical uncertainties appear to be of secondary importance when compared to the large amount of scatter present in observations of ^{7}Be in nova ejecta.

The authors wish to thank the anonymous referee for their helpful feedback. A.R.C. is supported in part by the Australian Research Council through a Discovery Early Career Researcher Award (DE190100656). B.C. acknowledges support from the National Science Foundation (NSF, USA) under grant No. PHY-1430152 (JINA Center for the Evolution of the Elements). R.G.I. thanks the STFC for funding, in particular Rutherford fellowship ST/L003910/1 and consolidated grant ST/R000603/1. Parts of this research were supported by the Australian Research Council Centre of Excellence for All Sky Astrophysics in 3 Dimensions (ASTRO 3D), through project number CE170100013.

Appendix
Key Features of the Nova Population: Ejecta Mass

Most of the key features of our nova populations are discussed in Kemp et al. (2021, 2022), who discuss which binary systems produce the most novae. However, the key features and distributions of nova properties when considering which systems produce the most nova ejecta require a brief description.

The relative importance of different WD masses in terms of the number of novae they produce is a balance between the initial mass function, which disfavors high-mass WD systems, and the increased rate at which these systems can produce novae because of their higher surface gravity and lower critical ignition masses (the mass of accreted material required for a nova eruption to occur).

However, reducing the critical ignition mass also reduces the mass of ejecta, which is further complicated by the question of accretion efficiency (the fraction of accreted material that is retained by the WD beyond the outburst). Increasing the WD mass can lead to higher accretion efficiencies (Wang 2018), further reducing the ejecta mass per eruption, but this effect is of secondary importance to the reduced critical ignition mass.

As shown in Figure 1, comparing the ejecta delay-time distributions to their delay-time counterparts reveals that late-time ejecta-mass contributions are significantly higher than when considering the raw nova rate. This is because the more massive O/Ne WDs contribute far less ejecta per event than their low-mass C/O WD counterparts, reducing the relative importance of their contributions to the distribution.

In general, nova systems that require high ($M_{\rm ig} \gtrsim 5 \times 10^{-5}$ $M_{\odot}$) critical ignition masses for outburst—typically characterized by low-mass WDs ($M_{\rm WD} < 0.8$ $M_{\odot}$) without extremely high accretion rates ($\dot{M} \lesssim 10^{-7}$ $M_{\odot}\,{\rm yr}^{-1}$)—dominate in terms of the mass of nova-processed material. High-mass ($M_{\rm WD} > 1$ $M_{\odot}$) WD systems are significantly less important when considering the ejecta mass. However, this does not preclude high-mass WDs contributing at a level comparable to or even higher than low-mass WDs when it comes to the nucleosynthesis of specific isotopes. The higher temperatures obtainable in nova eruptions on massive WDs offer unique nucleosynthetic pathways leading to a far more efficient synthesis of elements with mass numbers higher than F, an effect able to outweigh their lower ejecta masses and system birth rates.

ORCID iDs

Alex J. Kemp https://orcid.org/0000-0003-2059-5841
Amanda I. Karakas https://orcid.org/0000-0002-3625-6951
Andrew R. Casey https://orcid.org/0000-0003-0174-0564
Benoit Côté https://orcid.org/0000-0002-9986-8816
Zara Osborn https://orcid.org/0000-0001-5546-6869

References

Arai, A., Tajitsu, A., Kawakita, H., & Shinnaka, Y. 2021, ApJ, 916, 44
Arnould, M., & Norgaard, H. 1975, A&A, 42, 55
Asplund, M., Grevesse, N., Sauval, A. J., & Scott, P. 2009, ARA&A, 47, 481
Bath, G. T., & Shaviv, G. 1978, MNRAS, 183, 515
Bensby, T., & Lind, K. 2018, A&A, 615, A151
Buder, S., Asplund, M., Duong, L., et al. 2018, MNRAS, 478, 4513
Buder, S., Sharma, S., Kos, J., et al. 2021, MNRAS, 506, 150
Cameron, A. G. W., & Fowler, W. A. 1971, ApJ, 164, 111
Cescutti, G., & Molaro, P. 2019, MNRAS, 482, 4372
Côté, B., O'Shea, B. W., Ritter, C., Herwig, F., & Venn, K. A. 2017, ApJ, 835, 128
Côté, B., Silvia, D. W., O'Shea, B. W., Smith, B., & Wise, J. H. 2018, ApJ, 859, 67
D'Antona, F., & Matteucci, F. 1991, A&A, 248, 62
Fryxell, B., Olson, K., Ricker, P., et al. 2000, ApJS, 131, 273
Fu, X., Romano, D., Bragaglia, A., et al. 2018, A&A, 610, A38
Gordon, A. C., Aydi, E., Page, K. L., et al. 2021, ApJ, 910, 134
Grisoni, V., Matteucci, F., Romano, D., & Fu, X. 2019, MNRAS, 489, 3539
Guiglion, G., de Laverny, P., Recio-Blanco, A., et al. 2016, A&A, 595, A18
Iliadis, C. 2015, Nuclear physics of stars (Wenheim: Wiley)
Izzard, R. G., Dray, L. M., Karakas, A. I., Lugaro, M., & Tout, C. A. 2006, A&A, 460, 565
Izzard, R. G., Glebbeek, E., Stancliffe, R. J., & Pols, O. R. 2009, A&A, 508, 1359
Izzard, R. G., Preece, H., Jofre, P., Halabi, G. M., Masseron, T., & Tout, C. A. 2018, MNRAS, 473, 2984
Izzard, R. G., Tout, C. A., Karakas, A. I., & Pols, O. R. 2004, MNRAS, 350, 407
Izzo, L., Della Valle, M., Mason, E., et al. 2015, ApJL, 808, L14
Izzo, L., Molaro, P., Cescutti, G., et al. 2022, MNRAS, 510, 5302
José, J., & Hernanz, M. 1998, ApJ, 494, 680
José, J., Shore, S. N., & Casanova, J. 2022, A&A, 634, A5
Karakas, A. I. 2010, MNRAS, 403, 1413
Kemp, A. J., Karakas, A. I., Casey, A. R., et al. 2021, MNRAS, 504, 6117
Kemp, A. J., Karakas, A. I., Casey, A. R., Kobayashi, C., & Izzard, R. G. 2022, MNRAS, 509, 1175
Kobayashi, C., Umeda, H., Nomoto, K., Tominaga, N., & Ohkubo, T. 2006, ApJ, 653, 1145
Lodders, K., Palme, H., & Gail, H. P. 2009, LanB, 4B, 712
Matteucci, F., D'Antona, F., & Timmes, F. X. 1995, A&A, 303, 460
Mena, E. D., de Lis, S. B., Adibekyan, V. Z., et al. 2015, A&A, 576, A69

Molaro, P., Izzo, L., Bonifacio, P., et al. 2020, MNRAS, 492, 4975
Molaro, P., Izzo, L., D'Odorico, V., et al. 2022, MNRAS, 509, 3258
Molaro, P., Izzo, L., Mason, E., Bonifacio, P., & Della Valle, M. 2016, MNRAS, 463, L117
Pignatari, M., Herwig, F., Hirschi, R., et al. 2016, ApJS, 225, 24
Prantzos, N. 2012, A&A, 542, A67
Romano, D., Matteucci, F., Ventura, P., & D'Antona, F. 2001, A&A, 374, 646
Rukeya, R., Lü, G., Wang, Z., & Zhu, C. 2017, PASP, 129, 074201
Selvelli, P., Molaro, P., & Izzo, L. 2018, MNRAS, 481, 2261
Starrfield, S., Bose, M., Iliadis, C., et al. 2020, ApJ, 895, 70
Starrfield, S., Iliadis, C., Hix, W. R., Timmes, F. X., & Sparks, W. M. 2009, ApJ, 692, 1532
Starrfield, S., Sparks, W., Truran, J., & Wiescher, M. 2000, ApJS, 127, 485
Starrfield, S., Truran, J. W., & Sparks, W. M. 1978, ApJ, 226, 186
Tajitsu, A., Sadakane, K., Naito, H., et al. 2016, ApJ, 818, 191
Tajitsu, A., Sadakane, K., Naito, H., Arai, A., & Aoki, W. 2015, Natur, 518, 381
Thielemann, F. K., Nomoto, K., & Yokoi, K. 1986, A&A, 158, 17
Wang, B. 2018, RAA, 18, 049
Wang, C., Jia, K., & Li, X.-D. 2016, RAA, 16, 126